

Electron-radiation interaction in a Penning trap: Beyond the dipole approximation

Ana M. Martins,¹ Stefano Mancini,² and Paolo Tombesi²

¹*Centro de Fisica de Plasmas, Instituto Superior Técnico, P-1096 Lisboa Codex, Portugal*

²*Dipartimento di Matematica e Fisica and Istituto Nazionale per la Fisica della Materia, Università di Camerino, I-62032 Camerino, Italy*

(Received 20 March 1998)

We investigate the physics of a single trapped electron interacting with a radiation field without the dipole approximation. This gives physical insights in the so-called geonium theory. [S1050-2947(98)04610-1]

PACS number(s): 42.50.Vk, 03.65.Bz, 42.50.Dv, 12.20.-m

I. INTRODUCTION

Simple systems such as a single electron or an ion provide a useful tool to investigate the fundamental laws of nature. Hence, in the past decades there has been increasing interest in trapping phenomena [1]. It is now routinely possible to trap a single ion [2], which would allow us to study quantum electrodynamics when the trapped ion interacts with a radiation mode. On the other hand, the electron stored in a Penning trap [3] permits accurate measurements too [4]. This system has been called a geonium atom since it resembles a hydrogen atom, for which the binding for the electron is to an external apparatus residing on the earth [5]. The geonium system was recently studied to implement some interesting quantum optics situations, such as quantum nondemolition measurements [6] and the generation of nonclassical states [7]. Here, 100 years after the discovery of the electron, we would show quantum features of a trapped electron interacting with the radiation field, when no dipole approximation is made. It is well known that in the geonium system [5] the motion of the electron can be separated into three independent harmonic motions: axial, cyclotron, and magnetron. It is also well established that entangled systems are extremely interesting for many purposes.

In the present work we propose a way of coupling the three harmonic oscillators of the geonium system by simply superposing a radiation field on the trapping fields. More concretely, we show that when the trapped electron oscillates in a standing wave field, there could be linear or nonlinear coupling among the axial motion and the other motions, although, in particular, we will consider only the axial-cyclotron interaction. Hence we shall present the more immediate consequences of such an entanglement, such as indirect measurements on the cyclotron mode. Then we shall investigate the generation of nonclassical features. Moreover, the analysis in all cases will be performed by taking into account the environmental effects as well.

The paper is organized as follows: Section II is devoted to the description of the model. The first-order (linear) coupling between axial and cyclotron motion is considered in Sec. III, while in Sec. IV the second-order coupling is discussed. In Sec. V we further discuss the possibility of generating nonclassical states. Finally, we present conclusions in Sec. VI.

II. MODEL

The geonium system consists [5] of an electron of charge e and mass m_0 moving in a uniform magnetic field \mathbf{B} , along

the positive z axis, and a static quadrupole potential

$$\hat{V} = V_0 \frac{\hat{x}^2 + \hat{y}^2 - 2\hat{z}^2}{4d^2}, \quad (1)$$

where d characterizes the dimension of the trap and V_0 is the potential applied to the trap electrodes [5]. In this work, in addition to the usual trapping fields, we embed the trapped electron in a radiation field of vector potential $\hat{\mathbf{A}}_{ext}$. To simplify our presentation, we assume the *a priori* knowledge of the electron spin [8]. Neglecting all spin-related terms, the Hamiltonian for the trapped electron can then be written as the quantum counterpart of the classical Hamiltonian

$$\hat{H} = \frac{1}{2m_0} \left[\hat{\mathbf{p}} - \frac{e}{c} \hat{\mathbf{A}} \right]^2 + e\hat{V}, \quad (2)$$

where c is the speed of light and

$$\hat{\mathbf{A}} = \frac{1}{2} \hat{\mathbf{r}} \times \hat{\mathbf{B}} + \hat{\mathbf{A}}_{ext}, \quad (3)$$

where $\hat{\mathbf{r}} \equiv (\hat{x}, \hat{y}, \hat{z})$ and $\hat{\mathbf{p}} \equiv (\hat{p}_x, \hat{p}_y, \hat{p}_z)$ are, respectively, the position and the conjugate momentum operators of the electron.

The motion of the electron in the absence of the external field $\hat{\mathbf{A}}_{ext}$ is the result of the motion of three harmonic oscillators [5]: the cyclotron, the axial and the magnetron, which are well separated in the energy scale (gigahertz, megahertz, and kilohertz, respectively). This can be easily understood by introducing the ladder operators

$$\hat{a}_z = \sqrt{\frac{m_0 \omega_z}{2\hbar}} \hat{z} + i \sqrt{\frac{1}{2\hbar m_0 \omega_z}} \hat{p}_z, \quad (4)$$

$$\hat{a}_c = \frac{1}{2} \left[\sqrt{\frac{m_0 \omega_c}{2\hbar}} (\hat{x} - i\hat{y}) + \sqrt{\frac{2}{\hbar m_0 \omega_c}} (\hat{p}_y + i\hat{p}_x) \right], \quad (5)$$

$$\hat{a}_m = \frac{1}{2} \left[\sqrt{\frac{m_0 \omega_c}{2\hbar}} (\hat{x} + i\hat{y}) - \sqrt{\frac{2}{\hbar m_0 \omega_c}} (\hat{p}_y - i\hat{p}_x) \right], \quad (6)$$

where the indices z , c , and m stand for axial, cyclotron, and magnetron respectively. The above operators obey the commutation relation $[\hat{a}_i, \hat{a}_i^\dagger] = 1$, $i = z, c, m$. The angular frequencies are given by

$$\omega_z = \sqrt{\frac{eV_0}{m_0 c d^2}}, \quad \omega_c = \frac{eB}{m_0 c}, \quad \omega_m \approx \frac{\omega_z^2}{2\omega_c}. \quad (7)$$

So when $\hat{\mathbf{A}}_{ext} = 0$, the Hamiltonian (2) simply reduces to

$$\hat{H} = \hbar \omega_z \left(\hat{a}_z^\dagger \hat{a}_z + \frac{1}{2} \right) + \hbar \omega_c \left(\hat{a}_c^\dagger \hat{a}_c + \frac{1}{2} \right) - \hbar \omega_m \left(\hat{a}_m^\dagger \hat{a}_m + \frac{1}{2} \right). \quad (8)$$

Instead, when the external radiation field is a standing wave along the z direction (with frequency Ω and wave vector k) and circularly polarized in the x - y plane [9], we have

$$\begin{aligned} \hat{\mathbf{A}}_{ext} = & \{ -i[\alpha e^{i\Omega t} - \alpha^* e^{-i\Omega t}] \\ & \times \cos(k\hat{z} + \phi), [\alpha e^{i\Omega t} + \alpha^* e^{-i\Omega t}] \cos(k\hat{z} + \phi), 0 \}. \end{aligned} \quad (9)$$

In such a case, for frequencies Ω close to ω_c , we can neglect the slow magnetron motion and the Hamiltonian (2) becomes

$$\begin{aligned} \hat{H} = & \hbar \omega_z \left(\hat{a}_z^\dagger \hat{a}_z + \frac{1}{2} \right) + \hbar \omega_c \left(\hat{a}_c^\dagger \hat{a}_c + \frac{1}{2} \right) \\ & + \hbar [\epsilon^* \hat{a}_c e^{i\Omega t} + \epsilon \hat{a}_c^\dagger e^{-i\Omega t}] \cos(k\hat{z} + \phi) \\ & + \hbar \chi \cos^2(k\hat{z} + \phi) \end{aligned} \quad (10)$$

where

$$\epsilon = |\epsilon| e^{i\varphi} = \left(\frac{2e^3 B}{\hbar m_0^2 c^3} \right)^{1/2} \alpha, \quad \chi = \frac{e^2}{\hbar m_0 c^2} |\alpha|^2, \quad (11)$$

and the phase φ is the phase of the applied radiation field (i.e., $\arg \alpha$). The other phase ϕ defines the position of the center of the axial motion with respect to the standing wave. The third and fourth terms on the right-hand side of the Hamiltonian (10) describe the nonlinear interaction between the trapped electron and the standing wave, which gives rise to a coupling between the axial and the cyclotron motion, whose effect will be analyzed in the following sections. In the usual Penning traps the quantity $k(\hat{z})$ can reach values up to approximately 0.1 [5], when $\Omega \approx \omega_c$. This leads us to explore the physics beyond the usual dipole approximation for the cosine term in Eq. (10). The cosine factor $\cos(k\hat{z} + \phi)$ can be split as

$$\cos(k\hat{z} + \phi) = \cos \phi \cos(k\hat{z}) - \sin \phi \sin(k\hat{z}) \quad (12)$$

and two typical situations corresponding to $\phi=0$ and $\phi = \pi/2$ can be easily exploited. By making the usual dipole approximation these two cases correspond to a mere driving term on the cyclotron motion ($\phi=0$) or to no effect at all ($\phi = \pi/2$).

In the following sections the behavior of the trapped electron in these two paradigmatic limits is studied. All the other possible values of ϕ will give rise to combinations of these two cases and can be easily studied. We further note that the last term in Eq. (10) can be neglected since the parameters (11) are such that $\chi/|\epsilon| \approx |\epsilon|/\omega_c$.

III. THE CASE OF $\phi = \pi/2$

In this section we consider the case $\phi = \pi/2$. Developing $\sin(k\hat{z})$ in a power series and keeping only the first-order term we can approximate the Hamiltonian (10) by

$$\begin{aligned} \hat{H} = & \hbar \omega_z \left(\hat{a}_z^\dagger \hat{a}_z + \frac{1}{2} \right) + \hbar \omega_c \left(\hat{a}_c^\dagger \hat{a}_c + \frac{1}{2} \right) \\ & + \hbar [\epsilon^* \hat{a}_c e^{i\Omega t} + \epsilon \hat{a}_c^\dagger e^{-i\Omega t}] k \hat{z}. \end{aligned} \quad (13)$$

In the case of perfect resonance $\Omega = \omega_c$ and in a frame rotating at that angular frequency we get the solution

$$\begin{aligned} \hat{z}(t) = & [\hat{z}(0) - |\epsilon| k \hat{X}_\varphi] \cos(\omega_z t) \\ & + \frac{1}{m \omega_z} \hat{p}_z(0) \sin(\omega_z t) + |\epsilon| k \hat{X}_\varphi, \end{aligned} \quad (14)$$

$$\hat{p}_z(t) = \hat{p}_z(0) \cos(\omega_z t) - m \omega_z [\hat{z}(0) - \sqrt{2} |\epsilon| k \hat{X}_\varphi] \sin(\omega_z t), \quad (15)$$

where we have introduced the cyclotron quadrature

$$\hat{X}_\varphi = \frac{\hat{a}_c e^{i\varphi} + \hat{a}_c^\dagger e^{-i\varphi}}{\sqrt{2}}. \quad (16)$$

Equation (15) suggests an indirect way to determine the probability distribution for the cyclotron quadrature $\mathcal{P}(X_\varphi)$. We recall that in the geonium system the measurements are performed only on the axial degree of freedom due to the nonexistence of good detectors in the microwave regime. The oscillating charged particle induces alternating image charges on the electrodes, which in turn cause an oscillating current to flow through an external circuit. The current will be proportional to the axial momentum \hat{p}_z ; hence a measurement of this current will also give the value of the quadrature \hat{X}_φ . Measurements when the standing wave is ‘‘off’’ should be done preventively to set the initial conditions. Then repeated measurements lead to the desired statistics $\mathcal{P}(X_\varphi)$. If the procedure is further repeated for several values of the phase φ , we obtain the set of marginal probabilities $\mathcal{P}(X, \varphi)$, which allows the tomographic imaging of the quantum state of the cyclotron mode [10].

We now consider the effects of the thermal damping through the resistance of the external circuit connected with the measurement apparatus. In such a case the equations of motion for the axial degree of freedom become

$$\frac{d\hat{z}}{dt} = \frac{\hat{p}_z}{m_0}, \quad (17)$$

$$\frac{d\hat{p}_z}{dt} = -\omega_z^2 m_0 \hat{z} - \frac{\gamma_z}{m_0} \hat{p}_z - \sqrt{2} \hbar k |\epsilon| \hat{X}_\varphi + \hat{\xi}, \quad (18)$$

where the noise term $\hat{\xi}(t)$ is that of Johnson noise with expectation values $\langle \hat{\xi}(t) \rangle = 0$ and $\langle \hat{\xi}(t) \hat{\xi}(t') \rangle = 2 \gamma_z k_B T \delta(t - t')$, the damping constant γ_z is proportional to the readout resistor, k_B is the Boltzmann constant, and T is the equilibrium temperature.

By using the Fourier transforms, we immediately obtain

$$\tilde{p}_z(\omega) = \frac{\sqrt{2\hbar k}|\epsilon|\tilde{X}_\varphi(\omega) - \tilde{\xi}(\omega)}{\omega^2 - \omega_z^2 - i\omega\gamma_z/m_0}; \quad (19)$$

hence the correlation

$$\begin{aligned} & \langle \tilde{p}_z(\omega)\tilde{p}_z(-\omega) \rangle \\ &= \frac{2(\hbar k|\epsilon|)^2 \langle \tilde{X}_\varphi(\omega)\tilde{X}_\varphi(-\omega) \rangle + \langle \tilde{\xi}(\omega)\tilde{\xi}(-\omega) \rangle}{|\omega^2 - \omega_z^2 - i\omega\gamma_z/m_0|^2}. \end{aligned} \quad (20)$$

Equation (20) imposes some limits on the observability of nonclassical effects on the cyclotron motion; in fact, the added thermal noise should be much less than the cyclotron vacuum noise for the chosen frequency, i.e., $\gamma_z k_B T \ll (\hbar k|\epsilon|)^2$.

IV. THE CASE OF $\phi=0$

Let us consider now the case of $\phi=0$. Keeping only terms up to the second order in $k\hat{z}$, the Hamiltonian (10) reduces to

$$\begin{aligned} \hat{H} = & \hbar\omega_z \left(\hat{a}_z^\dagger \hat{a}_z + \frac{1}{2} \right) + \hbar\omega_c \left(\hat{a}_c^\dagger \hat{a}_c + \frac{1}{2} \right) \\ & + \hbar[\epsilon^* \hat{a}_c e^{i\Omega t} + \epsilon \hat{a}_c^\dagger e^{-i\Omega t}] \left[1 - \frac{k^2 \hat{z}^2}{2} \right], \end{aligned} \quad (21)$$

which clearly shows the nonlinear coupling as a consequence of the higher-order expansion with respect to the case of the preceding section. We study the general case including losses. The latter are present in the axial degree of freedom once the connection with the external circuit is established, as pointed out in Sec. III. Instead, the noise on the cyclotron degree of freedom could arise, e.g., from radiative damping (though it can be strongly reduced with an appropriate trap geometry).

Hence, by starting from the Hamiltonian (21), we obtain the quantum stochastic differential equations

$$\frac{d\hat{a}_c}{dt} = -i\Delta\hat{a}_c - \frac{\gamma_c}{2}\hat{a}_c - i\epsilon(1 - \kappa^2\hat{Z}^2) + \sqrt{\gamma_c}\hat{a}_c^{in}, \quad (22)$$

$$\frac{d\hat{a}_c^\dagger}{dt} = i\Delta\hat{a}_c^\dagger - \frac{\gamma_c}{2}\hat{a}_c^\dagger + i\epsilon^*(1 - \kappa^2\hat{Z}^2) + \sqrt{\gamma_c}[\hat{a}_c^{in}]^\dagger, \quad (23)$$

$$\frac{d\hat{Z}}{dt} = \omega_z\hat{P}_z, \quad (24)$$

$$\frac{d\hat{P}_z}{dt} = -\omega_z\hat{Z} + 2\kappa^2(\epsilon^*\hat{a}_c + \epsilon\hat{a}_c^\dagger)\hat{Z} + f - \frac{\gamma_z}{m_0}\hat{P}_z - \hat{\Xi}, \quad (25)$$

where $\Delta = \omega_c - \Omega$, f is a driving term for the axial motion, γ_c is the cyclotron damping constant, and $\hat{a}_c^{in}, \hat{\Xi}$ are the noise terms (we shall consider the situation where only the vacuum contributes to the cyclotron noise). We have introduced the scaled variables $\hat{Z} = \sqrt{m_0\omega_z/\hbar}\hat{z}$, $\hat{P}_z = \sqrt{1/\hbar m_0\omega_z}\hat{p}_z$, $\hat{\Xi} = \sqrt{1/\hbar m_0\omega_z}\hat{\xi}$, and $\kappa^2 = \hbar k^2/2m_0\omega_z$. From Eq. (25) we can see that the cyclotron quadrature causes a shift of the resonant frequency of the axial motion, so its indirect measurement is feasible.

The system of equations (22)–(25) can be linearized around the steady state [11]. The stationary values $\bar{\alpha}_c$, \bar{Z} , and \bar{P}_Z can be obtained from

$$0 = -\left(\frac{\gamma_c}{2} + i\Delta\right)\bar{\alpha}_c - i\epsilon(1 - \kappa^2\bar{Z}^2), \quad (26)$$

$$0 = -\left(\frac{\gamma_c}{2} - i\Delta\right)\bar{\alpha}_c^* + i\epsilon^*(1 - \kappa^2\bar{Z}^2), \quad (27)$$

$$0 = \omega_z\bar{P}_Z, \quad (28)$$

$$0 = -[\omega_z - 2\kappa^2(\epsilon^*\bar{\alpha}_c + \epsilon\bar{\alpha}_c^*)]\bar{Z} + f. \quad (29)$$

The linearized system is then

$$\frac{d}{dt} \begin{pmatrix} \hat{a}_c \\ \hat{a}_c^\dagger \\ \hat{Z} \\ \hat{P}_z \end{pmatrix} = \mathbf{M} \begin{pmatrix} \hat{a}_c \\ \hat{a}_c^\dagger \\ \hat{Z} \\ \hat{P}_z \end{pmatrix} + \begin{pmatrix} \sqrt{\gamma_c}\hat{a}_c^{in} \\ \sqrt{\gamma_c}[\hat{a}_c^{in}]^\dagger \\ 0 \\ -\hat{\Xi} \end{pmatrix}, \quad (30)$$

where now the operators indicate the quantum fluctuations with respect to the steady state and

$$\mathbf{M} = \begin{pmatrix} -\left(\frac{\gamma_c}{2} + i\Delta\right) & 0 & 2i\epsilon\kappa^2\bar{Z} & 0 \\ 0 & -\left(\frac{\gamma_c}{2} - i\Delta\right) & -2i\epsilon^*\kappa^2\bar{Z} & 0 \\ 0 & 0 & 0 & \omega_z \\ -2\epsilon^*\kappa^2\bar{Z} & -2\epsilon\kappa^2\bar{Z} & -\omega_z + 2\kappa^2(\epsilon^*\bar{\alpha}_c + \epsilon\bar{\alpha}_c^*) & -\frac{\gamma_z}{m_0} \end{pmatrix}. \quad (31)$$

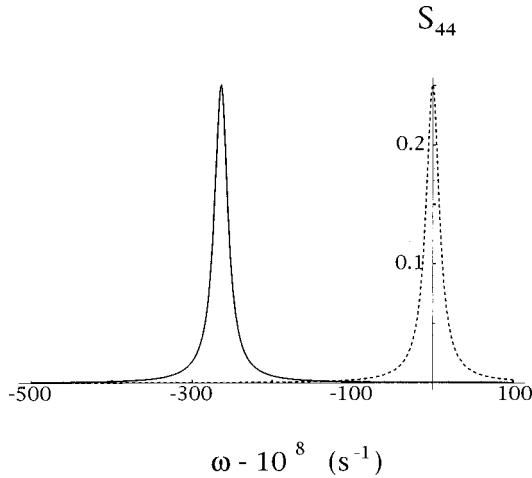


FIG. 1. Spectrum of axial momentum for $\Delta = 1.5 \times 10^4 \text{ s}^{-1}$, $\kappa^2 = 10^{-6}$, $\gamma_c = 1.5 \text{ s}^{-1}$, $\gamma_z/m_0 = 20 \text{ s}^{-1}$, $|\epsilon| = 1.4 \times 10^4 \text{ s}^{-1}$, $\varphi = 3\pi/4$, $f = 10^{11} \text{ s}^{-1}$, and $N_{th} = 10^3$. The peak on the right represents the resonance in the absence of coupling. The separation between peaks is proportional to the cyclotron quadrature amplitude.

The spectral matrix can be calculated as

$$\mathbf{S}(\omega) = (i\omega\mathbf{I} - \mathbf{M})^{-1} \mathbf{D} (-i\omega\mathbf{I} - \mathbf{M}^T)^{-1}, \quad (32)$$

where \mathbf{I} is the 4×4 identity matrix, the superscript T denotes the transpose, and

$$\mathbf{D} = \begin{pmatrix} 0 & \gamma_c & 0 & 0 \\ 0 & 0 & 0 & 0 \\ 0 & 0 & 0 & 0 \\ 0 & 0 & 0 & \frac{\gamma_z}{m_0} N_{th} \end{pmatrix}, \quad (33)$$

with $N_{th} = k_B T / \hbar \omega_z$ the number of thermal excitations.

The momentum correlation for the axial motion will be \mathbf{S}_{44} ; this quantity is plotted in Fig. 1. The dashed line represents the resonance in the absence of coupling and the solid line the resonance in the presence of it. The separation between peaks is proportional to the cyclotron quadrature amplitude. So it gives us an indirect value of that cyclotron observable.

Furthermore, the variance for the amplitude cyclotron quadrature is given by integrating the quantity $\mathbf{S}_{11} + \mathbf{S}_{22} + \mathbf{S}_{12} + \mathbf{S}_{21}$, which is plotted in Fig. 2 (dashed line). The figure also shows the variance for the orthogonal quadrature (solid line). It can be seen that the system exhibits squeezing effects depending on the detuning. It is worth noting that such effects are not very sensitive to thermal noise. The stability of the system, for the values of parameters used, is checked through the signs of the eigenvalues of the matrix \mathbf{M} .

In this section and Sec. III we have shown that the terms beyond the dipole approximation could play an important role and should not be neglected abruptly. As a matter of fact, we have presented a variety of effects (see, e.g., Figs. 1 and 2) that could be measured in common Penning traps. In the following, we shall explore other possibilities.

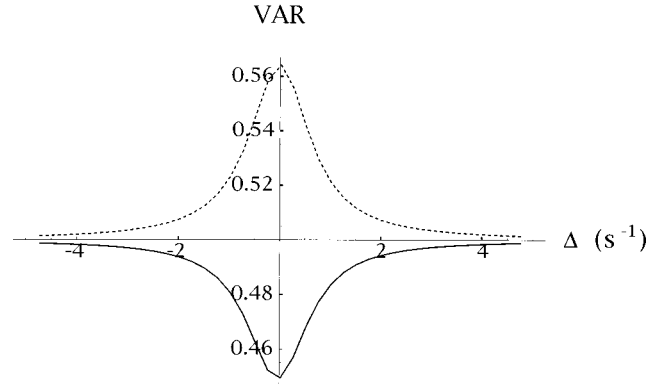


FIG. 2. Variance for the cyclotron quadratures $X_{\varphi=0}$ (dashed line) and $X_{\varphi=\pi/2}$ (solid line) as a function of the detuning Δ . The values of other parameters are the same as in Fig. 1.

V. NONCLASSICAL STATES

We now demonstrate the generation of nonclassical effects due to the nonlinearity induced by the Hamiltonian (21).

A. Central resonance

If we tune the standing wave at frequency $\Omega = \omega_c$ and pass to the interaction picture, the Hamiltonian (21) simply becomes

$$\hat{H} = \sqrt{2} \hbar |\epsilon| \hat{X}_c \left[1 - \kappa^2 \left(\hat{a}_z^\dagger \hat{a}_z + \frac{1}{2} \right) \right], \quad (34)$$

where we have disregarded the rapidly oscillating terms $\hat{a}_z^\dagger e^{-2i\omega_z t}$ and $\hat{a}_z e^{2i\omega_z t}$ (i.e., we made the rotating wave approximation). Starting from initial coherent states for both modes

$$|\Psi(0)\rangle = |\alpha\rangle_c \otimes |\beta\rangle_z, \quad (35)$$

we obtain from the Hamiltonian (34) the state at the time t ,

$$|\Psi(t)\rangle = e^{-|\beta|^2/2} \sum_{n=0}^{\infty} \frac{\beta^n}{\sqrt{n!}} |\theta_n t\rangle_c \otimes |n\rangle_z, \quad (36)$$

where $\theta_n = i\epsilon\kappa^2 n$. In writing the state (36) we have disregarded, for the sake of simplicity, the quantity $\alpha - i\epsilon(1 - \kappa^2/2)t$, which is common to each cyclotron component (this corresponds to an overall displacement in the cyclotron phase space).

Therefore, the electron motion evolves classically as a mixture of coherent states. Thus, during the evolution, no nonclassical states of the electron are generated. However, because of the entanglement between the cyclotron and the axial degrees of freedom, it is possible to generate nonclassical states of the cyclotron motion by performing conditional measurements on the axial degree of freedom. In particular, a measurement of the axial current corresponds to the projection onto an eigenstate $|p_z\rangle$ of the axial momentum

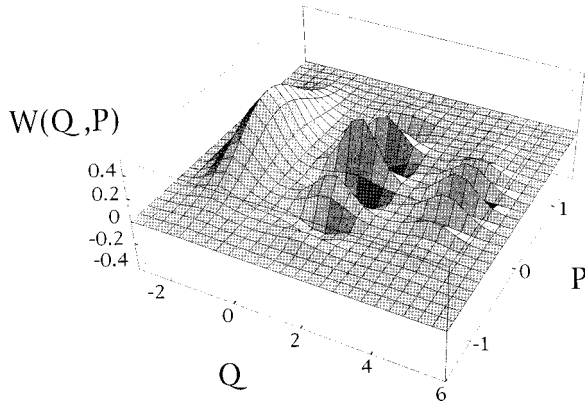


FIG. 3. Wigner function of Eq. (38) plotted for the parameters $\beta=1$ and $\epsilon\kappa^2t=-2.4i$, after an axial momentum measurement yielding the most probable value of p_z .

$$|\Psi(t)\rangle_{after} = \mathcal{N} \sum_{n=0}^{\infty} \left[e^{-|\beta|^2/2} \frac{\beta^n}{\sqrt{n!}} \langle p_z | n \rangle_z \right] |\theta_n t\rangle_c \otimes |p_z\rangle, \quad (37)$$

where \mathcal{N} is a normalization constant and $\langle p_z | n \rangle_z$ are the harmonic oscillator wave functions in momentum space. It is immediately seen from the above expression that after the measurement the system is left in a superposition of coherent cyclotronic states that could have nonclassical features. Whenever the number of coherent states that are being superposed is small, the states are known as Schrödinger cat states [12].

It is worth noting that the separation between the superposed coherent states is given by $|\epsilon|\kappa^2t$ and therefore it can be made truly macroscopic by emphasizing the nonclassicality (by simply requiring that $|\epsilon|\kappa^2t > 1$). However, one has to be careful when satisfying the above condition since it also implies a strong excitation of the cyclotron motion (the overall displacement that has been disregarded), which in turn could give rise to instabilities or even the loss of the particle over the trap's walls.

The Wigner function of the cyclotron state generated by conditional measurement can be written as

$$W(Q,P) = \mathcal{N}^2 \sum_{m,n} c_m^* c_n \exp \left[-Q^2 - P^2 - \frac{|\zeta_m|^2}{2} - \frac{|\zeta_n|^2}{2} + \sqrt{2}Q(\zeta_n + \zeta_m^*) - \sqrt{2}iP(\zeta_n - \zeta_m^*) - \zeta_n \zeta_m^* \right], \quad (38)$$

where the variables Q, P are associated with the quadratures $\hat{X}_{\varphi=0}$ and $\hat{X}_{\varphi=\pi/2}$, respectively, and

$$c_n = e^{-|\beta|^2/2} \frac{\beta^n}{\sqrt{n!}} \langle p_z | n \rangle_z, \quad (39)$$

$$\zeta_n = \theta_n t. \quad (40)$$

In Fig. 3 we present the Wigner function of the cyclotron state generated by the conditional measurement on the axial

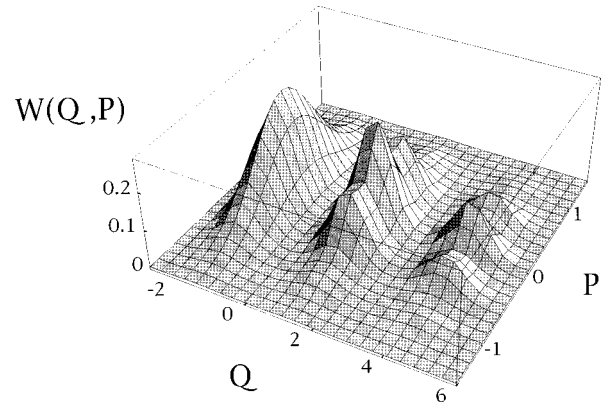


FIG. 4. Same as Fig. 3, but including the effects of the finite-time measurement. Here $\Gamma\tau=0.1$ and $N_{th}=10$.

degree of freedom. The negative parts and several oscillations show the nonclassicality of such a state.

We have considered the measurement process conditioning the cyclotron state as instantaneous; however, it always takes a finite time, during which the system undergoes the back action of the measurement apparatus. To take into account these effects we should adopt a precise Hamiltonian model describing the measurement of the observable \hat{p}_z . Nevertheless, from a phenomenological point of view, we can model the measurement process, performed on the state $\hat{\rho}(t) = |\Psi(t)\rangle\langle\Psi(t)|$, during a time τ , as the transition

$$\hat{\rho}(t) \rightarrow \text{Tr}_z[\hat{\rho}(t+\tau)|p_z\rangle\langle p_z|], \quad (41)$$

where $\hat{\rho}(t+\tau)$ is obtained from $\hat{\rho}(t)$ through free evolution in a thermal bath (representing the back action of the measurement apparatus on the system), while the projector indicates the output resulting at the end of the measurement [13].

To evaluate the effects of the measurement on the cyclotron state we should calculate the reduced density operator [the right-hand side of Eq. (41)]. Its corresponding Wigner function is derived in Appendix A as

$$W(Q,P,\tau) = \mathcal{N}^2 \sum_{m,n} \frac{\beta^m (\beta^*)^n}{m! n!} 2^{-(m+n)/2} I_{m,n} \times \exp \left[-Q^2 - P^2 - \frac{|\zeta_m|^2}{2} - \frac{|\zeta_n|^2}{2} + \sqrt{2}Q(\zeta_m + \zeta_n^*) - \sqrt{2}iP(\zeta_m - \zeta_n^*) - \zeta_m \zeta_n^* \right], \quad (42)$$

where

$$I_{m,n} = 2^n m! \int dv \exp \{ -[e^{-2\Gamma\tau} + 2N_{th}(1 - e^{-2\Gamma\tau})]v^2 - 2iP_z v \} \times (-ve^{-\Gamma\tau})^{n-m} L_m^{n-m}(2v^2 e^{-2\Gamma\tau}), \quad n > m, \quad (43)$$

with L_m^n the associated Laguerre polynomials and $\Gamma = \gamma_z/m_0$ the effective axial damping constant.

The Wigner function (42) is plotted in Fig. 4 and shows

the deleterious effects of finite-time measurement on the nonclassical state represented in Fig. 3. Of course, these effects strongly depend on the number of thermal excitations N_{th} as well. Once the cat states are generated by the conditional measurements, it would be possible to detect them by using indirect measurements as proposed in the previous sections.

B. The sideband resonance

We now return to the Hamiltonian (21) to consider another resonance, in this case $\Omega = (\omega_c - 2\omega_z) - \delta$, where δ is a small detuning (i.e., $\delta \ll \omega_z$) introduced for convenience. In a frame rotating at frequency $\omega_c - \delta$, we then have

$$\hat{H} = \hbar \delta \hat{a}_c^\dagger \hat{a}_c - \hbar \frac{|\epsilon| \kappa^2}{2} (\hat{a}_c \hat{a}_z^\dagger e^{-i\varphi} + a_c^\dagger a_z^2 e^{i\varphi}). \quad (44)$$

This is a trilinear Hamiltonian analogous to that studied in nonlinear optical processes such as parametric oscillation or second harmonic generation [11].

The equations of motion are

$$\frac{d\hat{a}_c}{dt} = -i\delta \hat{a}_c + i \frac{1}{2} |\epsilon| \kappa^2 \hat{a}_z^2, \quad (45)$$

$$\frac{d\hat{a}_z}{dt} = i |\epsilon| \kappa^2 \hat{a}_z^\dagger \hat{a}_c \quad (46)$$

and, by adiabatic elimination of the cyclotron mode, we get

$$\frac{d\hat{a}_z}{dt} = i \frac{|\epsilon|^2 \kappa^4}{2\delta} \hat{a}_z^\dagger \hat{a}_z^2. \quad (47)$$

This equation corresponds to an effective Hamiltonian for the axial motion of the type

$$\hat{H}_{eff} = -\hbar \frac{|\epsilon|^2 \kappa^4}{4\delta} (\hat{a}_z^\dagger)^2 \hat{a}_z^2, \quad (48)$$

which shows a well known Kerr-type nonlinearity. Hence we should expect nonclassical effects, such as Schrödinger cat states, when one starts from the initial conditions (35), also in the axial mode. In fact, the evolved axial state can be written as

$$|\psi(t)\rangle_z = \exp\{iG[(\hat{a}_z^\dagger \hat{a}_z)^2 - \hat{a}_z^\dagger \hat{a}_z]t\} |\beta\rangle_z, \quad G = \frac{|\epsilon|^2 \kappa^4}{4\delta}. \quad (49)$$

It is easy to show that after a time $t = \pi/2G$ the initial coherent state evolves into a cat state of the type discussed in Ref. [14],

$$|\psi(t = \pi/2G)\rangle = \frac{1}{\sqrt{2}} [e^{-i\pi/4} | -i\beta \rangle + e^{i\pi/4} | i\beta \rangle]. \quad (50)$$

This state shows interference in the phase space, which could be detected by measuring an appropriate quadrature. Therefore, by adjusting the initial conditions we may exploit the axial momentum measurement to see such interference. The Wigner function of the state (50) results,

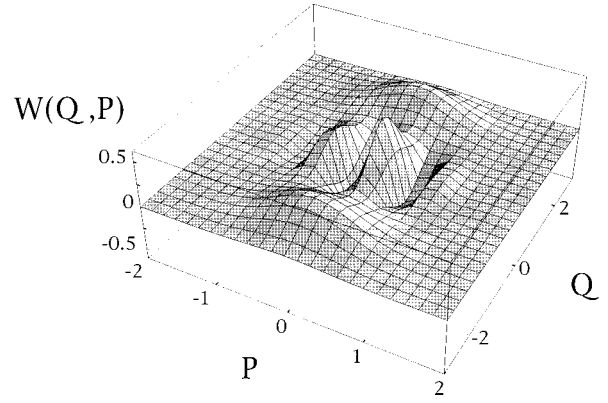


FIG. 5. Wigner function of the cat state (50) plotted for $\beta=2$.

$$\begin{aligned} W(Z, P_z) &= \frac{1}{\pi} e^{-|\beta|^2 - Z^2 - P_z^2} \\ &\times \{e^{-|\beta|^2} \cosh[2\sqrt{2}P_z \operatorname{Re}(\beta) - 2\sqrt{2}Z \operatorname{Im}(\beta)] \\ &+ e^{|\beta|^2} \sin[2\sqrt{2}P_z \operatorname{Im}(\beta) + 2\sqrt{2}Z \operatorname{Re}(\beta)]\}, \end{aligned} \quad (51)$$

and is represented in Fig. 5. The fact that only two coherent states are being superposed is evident from the two hills beside the central structure, which is different from the situation of Fig. 3, where more components contributes to the cat state.

Of course, we should deal again with the problem of measurement, whose process renders the system open and hence the dissipation tends to eliminate out the nonclassical effects. To evaluate this phenomenon we switch off the nonlinearity at the time of cat generation and a subsequent free evolution of the axial degree of freedom in a thermal bath, representing the effects of the external readout circuit. If the latter takes a time τ , we have (see Appendix B)

$$\begin{aligned} W(Z, P_z, \tau) &= \frac{1}{2} e^{-|\beta|^2 + \beta^2/2 + \beta^{*2}/2} \\ &\times \{e^{2\operatorname{Im}(\beta)^2} [I_1 + I_2] - ie^{-2\operatorname{Re}(\beta)^2} [I_3 - I_4]\}, \end{aligned} \quad (52)$$

where

$$I_i = \frac{2}{\pi \sqrt{4AB - C^2}} \exp\left[\frac{BD_i^2 + CD_i \mathcal{E}_i + A\mathcal{E}_i^2}{4AB - C^2}\right], \quad i = 1, 2, 3, 4, \quad (53)$$

with

$$\begin{aligned} A &= \frac{1}{\Gamma^2} (e^{-\Gamma\tau} - 1)^2 + 1 + 2\frac{N_{th}}{\Gamma^2} (1 - e^{-2\Gamma\tau}) \\ &- 8\frac{N_{th}}{\Gamma^2} (1 - e^{-\Gamma\tau}) + 4\frac{N_{th}}{\Gamma} \tau, \end{aligned} \quad (54)$$

$$B = e^{-2\Gamma\tau} + 2N_{th}(1 - e^{-2\Gamma\tau}), \quad (55)$$

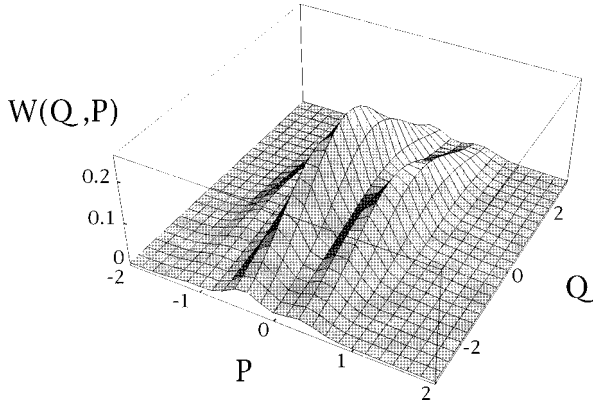


FIG. 6. Same as Fig. 5, but including the effects of the finite time measurement. Here $\Gamma=6$, $\tau=0.4$, and $N_{th}=10$.

$$\begin{aligned} C = & -\frac{2}{\Gamma} e^{-\Gamma\tau} (e^{-\Gamma\tau} - 1) - 4\frac{N_{th}}{\Gamma} (1 - e^{-2\Gamma\tau}) \\ & + 8\frac{N_{th}}{\Gamma} (1 - e^{-\Gamma\tau}), \end{aligned} \quad (56)$$

and

$$\mathcal{D}_2 = \mp 2\sqrt{2}i \operatorname{Im}(\beta) \mp \frac{\sqrt{2}}{\Gamma} i \operatorname{Re}(\beta) e^{-\Gamma\tau} \pm \frac{\sqrt{2}}{\Gamma} i \operatorname{Re}(\beta) + 2iZ, \quad (57)$$

$$\mathcal{D}_4 = \mp 2\sqrt{2} \operatorname{Re}(\beta) \pm \frac{\sqrt{2}}{\Gamma} \operatorname{Im}(\beta) e^{-\Gamma\tau} \mp \frac{\sqrt{2}}{\Gamma} \operatorname{Im}(\beta) + 2iZ, \quad (58)$$

$$\mathcal{E}_2 = \mp 2\sqrt{2}i \operatorname{Re}(\beta) e^{-\Gamma\tau} - 2iP_z, \quad (59)$$

$$\mathcal{E}_4 = \pm 2\sqrt{2} \operatorname{Im}(\beta) e^{-\Gamma\tau} - 2iP_z. \quad (60)$$

The Wigner function (52) is plotted in Fig. 6 and shows that the cat state (50) is very sensitive to the noise induced by the measurement.

VI. CONCLUSIONS

In conclusion, we have studied a trapped electron interacting with a standing radiation field and have shown that several interesting features can arise when the dipole approximation is not invoked. First, the proposed model provides a method for indirect measurement on the cyclotron degree of freedom. In addition, the possibilities to generate nonclassical states could be useful to test the linearity of quantum mechanics, [16] and to probe the decoherence of a mesoscopic system [17]. Furthermore, it is worth noting that the entanglement induced by the radiation field could also be used to explore the quantum logic possibilities of a trapped electron system.

Hence the geonium system in such a configuration could result as an alternative and/or a complement to other trapped systems. In addition, it has the advantage of involving a structureless particle, while, for example, an ion in a Paul trap behaves as a two-level system only ideally. Moreover, considering the electron as an antiparticle, the model could

also be used to perform some fundamental tests of symmetry.

Finally, based on these considerations, we conclude that it should be an interesting challenge to experimentally implement this model. The realistic values of the parameters (see, e.g., Ref. [5]) we have used yield that feasible with the actual technology. The main problem could be represented by the low values of N_{th} in Sec. IV; however, to better evidence the desired effects one could adjust the experimental setup in order to increase the inhomogeneity of the field experienced by the particle (to this end, we note that traps bigger than the usual ones are available as well [18]).

ACKNOWLEDGMENTS

A.M.M. would like to thank the University of Camerino for kind hospitality. S.M. would like to thank the Instituto Superior Técnico for kind hospitality and the INFN (Sezione Perugia) for partial support.

APPENDIX A

We consider the position space matrix elements of the state $\hat{\rho}(t)$, i.e.,

$${}_c\langle Q+Y|_z\langle Z'|\hat{\rho}(t)|Z''\rangle_z|Q-Y\rangle_c, \quad (A1)$$

and we denote them as $\wp(Z', Z'')$ since the evolution will take place only in axial space. The dependence on the cyclotron variables remains implicit. Then, with the aid of Eq. (36) we get

$$\wp(Z', Z'') = \sum_{m,n} C_m C_n^* \exp[-(Z'^2 + Z''^2)/2] H_m(Z') H_n(Z''), \quad (A2)$$

where H_m are the Hermite polynomials and

$$C_m = \left(\frac{1}{\pi}\right)^{1/4} \frac{1}{\sqrt{2^m m!}} e^{-|\beta|^2/2} \frac{\beta^m}{\sqrt{m!}} \langle Q+Y|\zeta_m\rangle, \quad (A3)$$

$$C_n^* = \left(\frac{1}{\pi}\right)^{1/4} \frac{1}{\sqrt{2^n n!}} e^{-|\beta|^2/2} \frac{(\beta^*)^n}{\sqrt{n!}} \langle \zeta_n|Q-Y\rangle. \quad (A4)$$

The master equation for the free evolution in a thermal bath [15] has the corresponding partial differential equation for the probability \wp

$$\begin{aligned} \partial_\tau \wp(Z', Z'') = & \left\{ \frac{i}{2} \left(\frac{\partial^2}{\partial Z'^2} - \frac{\partial^2}{\partial Z''^2} \right) \right. \\ & - \frac{\Gamma}{2} (Z' - Z'') \left(\frac{\partial}{\partial Z'} - \frac{\partial}{\partial Z''} \right) \\ & \left. - \Gamma N_{th} (Z' - Z'')^2 \right\} \wp(Z', Z''), \end{aligned} \quad (A5)$$

where we have set $\Gamma = \gamma_z/m_0$. Both the damping constant and the time are scaled by the axial frequency, i.e., $\Gamma/\omega_z \rightarrow \Gamma$ and $\tau\omega_z \rightarrow \tau$.

The differential equation (A5) is considerably simplified by the change of variables

$$Z' = u + v, \quad (\text{A6})$$

$$Z'' = u - v, \quad (\text{A7})$$

leading to

$$\partial_\tau \wp(u, v, \tau) = \left\{ \frac{i}{2} \frac{\partial^2}{\partial u \partial v} - \Gamma v \frac{\partial}{\partial v} - 4\Gamma N_{th} v^2 \right\} \wp(u, v, \tau). \quad (\text{A8})$$

By using the Fourier transform

$$\wp(u, v) = \int dq e^{2iqu} \tilde{\wp}(q, v), \quad (\text{A9})$$

Eq. (A8) becomes

$$\frac{\partial \tilde{\wp}}{\partial \tau} + (q + \Gamma v) \frac{\partial \tilde{\wp}}{\partial v} = -4\Gamma N_{th} v^2 \tilde{\wp}, \quad (\text{A10})$$

which can be solved by the method of characteristics. The solution takes the form

$$\begin{aligned} \tilde{\wp}(q, v, \tau) = & \tilde{\wp} \left\{ q, \left[\left(v + \frac{q}{\Gamma} \right) e^{-\Gamma \tau} - \frac{q}{\Gamma}, 0 \right] \right\} \\ & \times \exp \left\{ -2N_{th} \left(v + \frac{q}{\Gamma} \right)^2 (1 - e^{-2\Gamma \tau}) \right. \\ & \left. + \frac{8N_{th}}{\Gamma} q \left(v + \frac{q}{\Gamma} \right) (1 - e^{-\Gamma \tau}) \right\} e^{-4q^2 N_{th} \tau / \Gamma}. \end{aligned} \quad (\text{A11})$$

In our case, from Eqs. (A2), (A6), (A7), and (A9),

$$\begin{aligned} \tilde{\wp}(q, v, 0) &= \sqrt{\pi} \exp[-v^2 - q^2] \\ & \times \left\{ \sum_{m < n} C_m C_n^* 2^n m! (-v - iq)^{n-m} L_m^{n-m} [2(v^2 + q^2)] \right. \\ & + \sum_{m=n} |C_n|^2 2^n n! L_m [2(v^2 + q^2)] \\ & \left. + \sum_{m > n} C_m C_n^* 2^m n! (-v - iq)^{m-n} L_n^{m-n} [2(v^2 + q^2)] \right\}, \end{aligned} \quad (\text{A12})$$

results, where L_n^m indicates the associated Laguerre polynomials. Therefore, starting from the above expression, the solution (A11) can be easily constructed.

The Wigner function of the cyclotron state after a measurement giving the result p_z (or, equivalently, P_z) will be

$$\begin{aligned} W(Q, P, \tau) = & \mathcal{N}^2 \int dY \langle Q + Y | \\ & \times \langle P_z | \hat{\rho}(t + \tau) | P_z \rangle_z | Q - Y \rangle_c e^{-2iPY}, \end{aligned} \quad (\text{A13})$$

where \mathcal{N} is the normalization constant needed after the projection. By inserting identities in terms of the set of states $\{|u \pm v\rangle_z\}$, with the aid of the Fourier transform (A9) we get

$$W(Q, P, \tau) = \mathcal{N}^2 \int dY \int dv \tilde{\wp}(0, v, \tau) e^{-2ivP_z - 2iYP}. \quad (\text{A14})$$

The dependence on the cyclotron variables Q and Y is implicitly on \wp . Hence, by performing the integration one arrives at the expression (42).

APPENDIX B

If τ is the duration of the measurement, at the end of the measurement we have

$$\begin{aligned} W(Z, P_z, \tau) &= \frac{1}{\pi} \int dv \langle Z + v | \hat{\rho}_z(\tau) | Z - v \rangle e^{-2iP_z v} \\ &= \frac{1}{\pi} \int dv \wp(Z, v, \tau) e^{-2iP_z v} \\ &= \frac{1}{\pi^2} \int dv \int dq \tilde{\wp}(q, v, \tau) e^{-2iP_z v + 2iqZ}, \end{aligned} \quad (\text{B1})$$

where $\tilde{\wp}(q, v, \tau)$ is the same as in Eq. (A11), but with the initial condition determined by Eq. (50),

$$\begin{aligned} \tilde{\wp}(q, v, 0) = & \frac{1}{2} e^{-|\beta|^2 - q^2 - v^2 + \beta^2/2 + \beta^{*2}/2} \{ \exp[2 \operatorname{Im}(\beta)^2 - 2\sqrt{2}i \operatorname{Im}(\beta)q - 2\sqrt{2}i \operatorname{Re}(\beta)v] \\ & + \exp[2 \operatorname{Im}(\beta)^2 + 2\sqrt{2}i \operatorname{Im}(\beta)q + 2\sqrt{2}i \operatorname{Re}(\beta)v] - i \exp[-2 \operatorname{Re}(\beta)^2 - 2\sqrt{2} \operatorname{Re}(\beta)q + 2\sqrt{2} \operatorname{Im}(\beta)v] \\ & + i \exp[-2 \operatorname{Re}(\beta)^2 + 2\sqrt{2} \operatorname{Re}(\beta)q - 2\sqrt{2} \operatorname{Im}(\beta)v] \}. \end{aligned} \quad (\text{B2})$$

Thus, by performing the double integral in Eq. (B1) we get the expression (52).

- [1] W. Paul, Rev. Mod. Phys. **62**, 531 (1990).
- [2] See, e.g., lectures by C. Cohen-Tannoudji and W. D. Phillips on laser cooling of neutral atoms and lectures by H. Walther and R. Blatt on laser cooling of trapped ions, in *Fundamental Systems in Quantum Optics*, 1990 Les Houches Lectures Session LIII, edited by J. Dalibard, J. M. Raimond, and J. Zinn-Justin (North-Holland, Amsterdam, 1992).
- [3] F. M. Penning, Physica (Amsterdam) **3**, 873 (1936).
- [4] R. S. Van Dyck, Jr., P. B. Schwinberg, and H. G. Dehmelt, in *Atomic Physics 9*, edited by R. S. Van Dyck, Jr. and E. N. Fortson (World Scientific, Singapore, 1984).
- [5] L. S. Brown and G. Gabrielse, Rev. Mod. Phys. **58**, 233 (1986).
- [6] I. Marzoli and P. Tombesi, Europhys. Lett. **24**, 515 (1993).
- [7] S. Mancini and P. Tombesi, Phys. Rev. A **56**, R1679 (1997).
- [8] G. Gabrielse, H. Dehmelt, and W. Kells, Phys. Rev. Lett. **54**, 537 (1985).
- [9] There can be some limiting conditions on the existence of such waves due to the trap electrodes; however, one can develop the same theory for other geometries, such as cylindrical traps [see, e.g., G. Gabrielse and J. Tan, in *Cavity Quantum Electrodynamics*, edited by P. R. Berman (Academic, London, 1994)].
- [10] S. Mancini and P. Tombesi, Phys. Rev. A **56**, 3060 (1997).
- [11] See, e.g., D. F. Walls and G. J. Milburn, *Quantum Optics* (Springer, Berlin, 1994).
- [12] E. Schrödinger, Naturwissenschaften **23**, 807 (1935); **23**, 823 (1935); **23**, 844 (1935).
- [13] The projector in Eq. (41) should be, in reality, a projector on an interval of values for p_z that accounts for the uncertainty arising by relating the electric current at the readout circuit with the axial observable. However, here, for simplicity, we are not considering the dynamics of the readout apparatus [a detailed treatment of this subject in terms of input-output theory is given by I. Marzoli, M.S. thesis, University of Camerino, 1992 (unpublished)].
- [14] B. Yurke and D. Stoler, Phys. Rev. Lett. **57**, 13 (1986).
- [15] C. W. Gardiner, *Quantum Noise* (Springer, Berlin, 1991).
- [16] S. Weinberg, Phys. Rev. Lett. **62**, 485 (1989).
- [17] W. H. Zurek, Phys. Today **44** (10), 36 (1991).
- [18] See, e.g., J. Eades *et al.*, CERN Report No. PSSC/89-15, p. 118, 1989 (unpublished).